THE ASTROPHYSICAL JOURNAL, 314:103–110, 1987 March 1

X-RAY STUDIES OF THE SUPERNOVA REMNANT N132D. I. MORPHOLOGY

JOHN P. HUGHES
Harvard-Smithsonian Center for Astrophysics
Received 1986 May 23; accepted 1986 August 25

ABSTRACT

From studies of the X-ray image of the supernova remnant N132D in the Large Magellanic Cloud, we determine that the supernova explosion occurred within a cavity in the interstellar medium. As a possible explanation for the formation of such a cavity we consider the H II region of the precursor star, which gives an adequate fit if the precursor stellar type is later than B0. We also derive limits on the age and explosion energy, assuming the applicability of the Sedov solution. These values, $2.3 \leq E(10^{51}$ ergs$) \leq 11.4$ and $4300 \leq t(\mathrm{yr}) \leq 7200$, are somewhat high but would be lower for the evolutionary scenario proposed here. In particular, consistency with the dynamical age estimates from the high-velocity oxygen-rich optical filaments (Lasker) can be obtained with a cavity density of ~ 0.01 cm^{-3} or less and an explosion energy of $\sim 10^{51}$ ergs. We determine the fraction ($\sim 10\%$) of the total emission which comes from the central regions of the remnant (presumably stellar ejecta) and compare it to the fraction (6%–10%) of emission in the O VIII Lyα line.

Subject headings: galaxies: Magellanic Clouds — nebulae: supernova remnants — X-rays: sources

I. INTRODUCTION

The supernova remnant (SNR) N132D in the Large Magellanic Cloud (LMC) is a well-studied object with several notable characteristics. It belongs to a small class of remnants, such as Cassiopeia A in our own galaxy, which exhibits optical emission lines of oxygen corresponding to expansion velocities of ~ 1000 km s^{-1} or more with relative intensities which imply a large overabundance of oxygen. It has a complex morphology with several components: the high-velocity oxygen-rich ring mentioned above, a larger limb-brightened shell of more normal composition, and finally a much larger diffuse region of optical emission only apparent toward the north (Lasker 1978).

In the X-ray band (0.2–4 keV) this object is also remarkable. It is the brightest LMC SNR at these wavelengths, and furthermore, high-dispersion spectroscopy reveals the presence of a strong emission line of O VIII Lyα, contributing a significant fraction to the total observed X-ray flux. Morphologically the X-rays are similar to the optical with the exception that the large diffuse region of optical emission toward the north does not appear in the X-ray image. In this paper we present an analysis of the X-ray image in which we demonstrate that the outer shell of emission (i.e., the second component mentioned above) arises from the propagation of the supernova (SN) blast wave into the walls of a cavity in the interstellar medium (ISM). We discuss possible modes of formation for the cavity and find an adequate qualitative fit if we postulate the existence of an H II region during the life of the precursor star, constrained to be later than B0.

The paper is organized as follows. A presentation of the X-ray observations carried out by the *Einstein Observatory* appears in § II. We also derive (model-dependent) values for the energy of the SN explosion as well as the remnant's age in this section. A detailed analysis of the X-ray image, focusing first on the outer shell emission and then on the emission from the central regions is in § III. In the final section we give some concluding remarks.

II. OBSERVATIONS

An extensive series of X-ray observations of N132D utilizing all the instruments on the *Einstein Observatory* were carried out between 1979 and early 1981. These observations are in many ways complimentary and include imaging data as well as spectral data ranging over more than one order of magnitude in X-ray bandpass and spectral resolutions. Below we discuss the various observations.

The lowest resolution ($\Delta E/E \approx 1$) but largest dynamic range (0.2 keV–4 keV) spectral observations were carried out by the imaging proportional counter (IPC). This instrument was pointed at N132D twice, once on 1979 April 12 and again on 1981 January 27 for effectively 1240 s and 2930 s, respectively. Unfortunately, the data from the second pointing were unusable because of discharging in the counter.[1] Spectral analysis of the first observation using Raymond and Smith (1977, 1986, private communication) collisional equilibrium ionization (EQI) thermal plasmas yields temperatures of $10^{6.8}$–$10^{7.1}$ K and hydrogen column densities of $10^{21.5}$–10^{21} cm^{-2}, corresponding to (unabsorbed) source luminosities (0.2–4 keV) of 7.5–4.5×10^{37} ergs s^{-1} at the LMC (55 kpc). Because of its small size ($\sim 80''$) N132D was spatially unresolved in the IPC and the spectral parameters quoted above are global averages over the remnant; no spatially resolved X-ray spectra are available.

Higher spectral resolution data were obtained by the solid state spectrometer (SSS) and the focal plane crystal spectrometer (FPCS) during 1979 and 1980. The SSS data were analyzed (Clark *et al.* 1982) in the usual manner, using two different temperature collisional ionization equilibrium thermal plasmas and adjustable elemental abundances. These authors find $T = 10^{6.82}$ K for the lower temperature component, a column density of 10^{21} H atoms cm^{-2}, and generally lowered metal abundances relative to solar. The FPCS generated one of the most exciting observations of this remnant, viz., a remarkably bright O VIII Lyα line (0.011 ± 0.001 photons cm^{-2} s^{-1}; Canizares 1985), contributing 6%–10% of the total X-ray flux from N132D. This line, falling at ~ 650 eV, becomes

[1] This was an infrequent failure of the IPC and was perhaps the result of the high gain of the counter during this pointing (BAL $\approx$ 19). The signature of the effect was a rapid aperiodic variation in the count rate of N132D, a consequence of the "shorting out" of the high voltage during the discharge which occurred elsewhere in the counter.

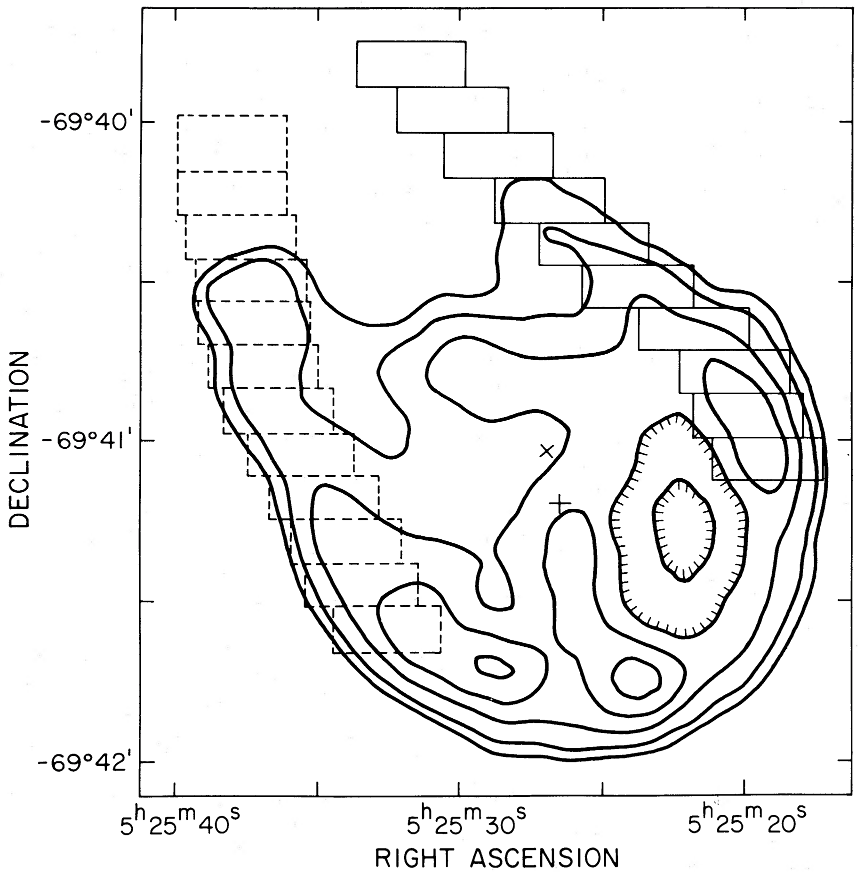

FIG. 1.—Contour plot of SNR N132D obtained by the HRI on *Einstein*. Gaussian smoothing ($\sigma = 4''$) has been applied. Contour levels are 0.2, 0.3, 0.5, 0.7, and 0.9 counts s^{-1} $arcmin^{-2}$. Note the local minimum in surface brightness toward the southwest; i.e., hatched contours. Average surface brightnesses were determined within each of the boxed regions for use in Fig. 2. The plus sign (+) marks the center of the spherical region, and the cross (×) marks the approximate center of the high-velocity oxygen-rich ring (Lasker 1980).

quite important in determining the emission in each of the other instruments, i.e., IPC, SSS, and the high-resolution imager (HRI). Another important constraint comes from an analysis of the Ne IX Heα and Ne X Lyα lines which implies an electron temperature of $\sim 10^{6.8}$ K and an ionization time scale $n_e t \approx 10^{11.4}$ cm^{-3} s (Markert *et al.* 1984). We leave a detailed discussion of these spectra to a future paper.

The final piece of spectral data comes from the monitor proportional counter (MPC), a nonimaging counter co-aligned with the axis of *Einstein* with eight spectral channels and energy range $\sim$1–20 keV. For thermal sources this data has only limited use and for N132D only the first four channels contain any statistically significant signal. Nevertheless, fits to thermal bremsstrahlung spectra (including gaunt factors) yield $T \approx 10^{6.9}$ K and column densities $\sim 10^{21.3}$ or less atoms cm^{-3}. One might expect somewhat higher column densities if Raymond and Smith thermal plasmas were used, because of the increased emission from lines at lower energies.

Finally we turn to the HRI observations performed on 1979 July 18. The effective exposure time was 8800 s, and the total source count rate was 1.30 ± 0.01 s^{-1} (statistical error only). A contour plot of the image (Fig. 1 and Mathewson *et al.* 1983)[2] clearly shows a limb-brightened shell with a marked degree of symmetry toward the southwest as well as a "blowout" to the northeast. There is also emission from the central region of the remnant, which seems to consist of two parts: (1) a region aligned approximately east-west slightly north of center and (2) a region southwest of this aligned $\sim 155°$ east of north. We will discuss the emission from the central regions in some detail later (§ III*b*).

The center of the symmetric region was determined by superposing various radii circles on the data and "eyeballing" the approximate best fit. Radial profiles of surface brightness in different azimuthal sectors (40° in size) were then constructed using that center and analyzed to determine radii and emitting densities (see below). Over the symmetric region ($\sim$140°–360°) the derived radii from the profiles are about the same at $\sim 44''$, corresponding to a radius of 11.7 pc for the LMC, and confirming our choice of center.

Two types of models were fitted to the surface brightness profiles: (1) an isothermal constant density shell of emission, with variable inner and outer shell radii, and (2) a Sedov (1959) profile of temperature and density (see Cox and Franco 1981 for an analytic approximation to the variation of these quantities in the interior of a Sedov SNR) with shock temperature and radius as variables. Each trial model was projected onto the plane of the sky, convolved with a circular Gaussian ($\sigma = 3''$) to approximate the spatial response of the HRI, and compared to the data. A grid search over the model variables (either inner and outer shell radius or shock radius and

[2] The contour plot of this object in Mathewson *et al.* (1983) is misleading since it does not mark the local minimum in surface brightness in the southwest.

TABLE 1

PARAMETERS FROM FITS TO HRI SURFACE BRIGHTNESS PROFILES OF N132D

	Isothermal Shell			Sedov Profile		
Angle (1)	R_i (2)	R_o (3)	$n(\mathrm{cm}^{-3})$ (4)	R_s (5)	$\log_{10} T_s$ (6)	$n(\mathrm{cm}^{-3})$ (7)
100[a]	39″	50″	3–4	47″	6.8	7–10
140..........	34	45	4–5	42	6.8	9–12
180..........	31	46	3–4	42	6.8	9–12
220..........	40	44	6–7	44	6.9	8–10
260..........	42	43	9–12	44	7.1	7–9
300..........	40	44	6–8	44	6.9	8–11
340[a]	33	52	2–3	48	6.8	6–8

[a] These are at the angular extremes of the symmetric region and hence contain emission from a range of radii. Consequently, the derived shell thicknesses are larger and the densities are smaller than corresponding values from the symmetric region.

temperature) was carried out to minimize χ^2. The results are shown in Table 1. The density values in columns (4) and (7) were derived from normalizing the model to the data profile in the following manner. The surface brightness for the isothermal shell can be expressed as

$$\Sigma = n^2 \Lambda(T, N_H) l \,, \tag{1}$$

where l is the line of sight through the shell (determined by geometric fits to the HRI data), $\Lambda(T, N_H)$ is the intrinsic luminosity in the HRI of an EQI plasma at temperature T for column density N_H (ranges on T and N_H are determined by the IPC data), Σ is the observed surface brightness, and n is the density of the emitting plasma. Clearly, normalizing the model to the observed surface brightness directly yields a value for the density. In the Sedov model equation (1) generalizes to an integral over Λ for different temperatures and line of sight distances; in this case the variation of derived density comes only from the range of N_H.

It is clear that the remnant has interacted with considerable amounts of mass. A preshock density range of 2–3 cm^{-3} as indicated by Table 1 implies a mass of 300–500 $M_\odot$ within the $\sim$12 pc radius of the remnant, leaving no doubt that the outer shell of emission arises from the motion of a blast wave through the ISM. We can use our observational values for radius, temperature, and density in conjunction with the Sedov theory (1959) for the motion of a blast wave in a homogeneous medium to determine limits on the age and energy of the SN explosion. The relevant equations are

$$R = 13(E_{51}/n)^{1/5} t_4^{2/5} \text{ pc} \,, \tag{2}$$

and

$$T = 0.33 \times 10^7 (E_{51}/n)^{2/5} t_4^{-6/5} \text{ K} \,, \tag{3}$$

where $E_{51} = E/10^{51}$ ergs and $t_4 = t/10^4$ yr. Immediately one sees that the age of the remnant t depends only on the radius and temperature as $t_4 = (R/13 \text{ pc})(T/0.33 \times 10^7 \text{ K})^{-1/2}$. This sets a density-independent range of $4300 \leq t(\mathrm{yr}) \leq 7200$ on the remnant's age using the measured temperature range $[10^{6.8} \leq T(\mathrm{K}) \leq 10^{7.1}]$ and a rather generous range on the radius $11 \leq R(\mathrm{pc}) \leq 13$. The radius uncertainty arises mostly from the distance uncertainty to the LMC plus the thickness of the cloud itself: we take 10% as the total uncertainty. This is actually much better than the radius estimate for most galactic remnants, which often are uncertain by factors of 2. Limits on the explosion energy can be determined by plotting equations (2)–(3) (solved for E as a function of t) for the various values of R, T, and n derived above. This is shown in Figure 2, where the

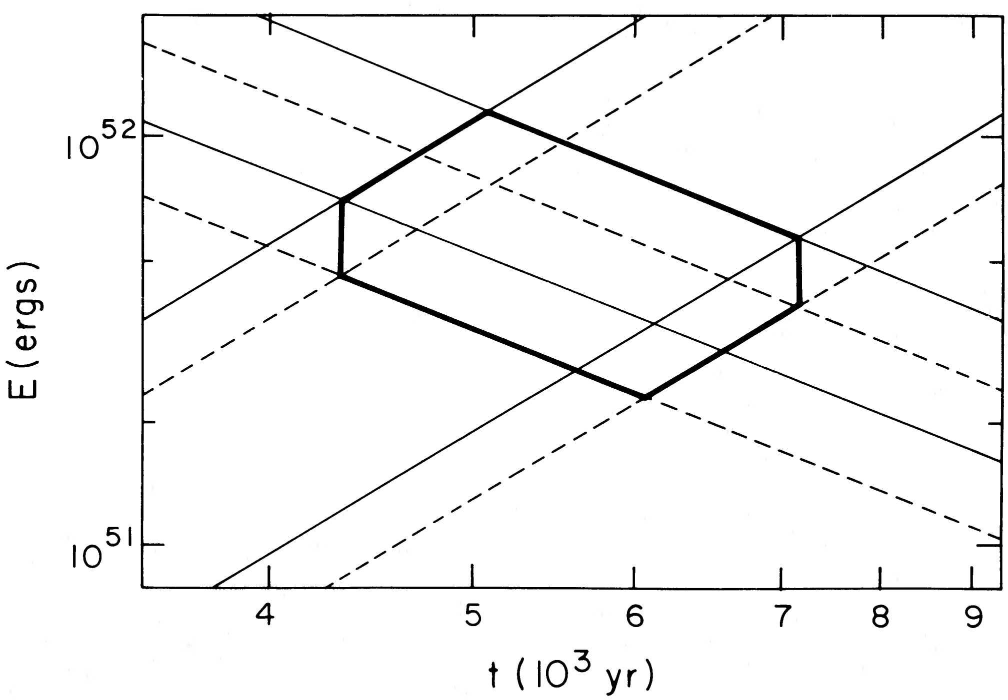

FIG. 2.—Plots of energy vs. age for the constraint equations on radius and temperature for SNRs in the Sedov approximation. The thin solid/dashed curves are for homogeneous ISM densities of 3 cm^{-3} (2 cm^{-3}). Positive slope curves arise from the temperature constraint equation ($T = 10^{7.1}$ K for the upper and $T = 10^{6.8}$ K for the lower); negative slope curves come from the radius constraint ($R = 13$ pc upper and $R = 11$ pc lower). The bold lines outline the allowed region of E vs. t for the given range of parameters.

curves with positive slope come from equation (3) for the shock temperature and the negative slope curves are from equation (2) for the radius. The thin solid/dashed lines correspond to a density of 3 cm^{-3} (2 cm^{-3}). The range of energy values so derived is $2.3 \leq E(10^{51}$ ergs) ≤ 11.4, large values even if the explosion was a type II.

The age derived above is considerably larger than the ~ 1300 yr age estimate of Lasker (1980) based on his analysis of the oxygen-rich filaments. There are several possible explanations for this. First, it might be that the central oxygen-rich filaments and the outer shell of emission are two physically unrelated SNRs which just happen to lie along the same line of sight. This is highly unlikely. There are only 10 SNRs (out of 30) in the LMC which are smaller than N132D (Hughes 1984). The probability of a chance superposition of any of these smaller SNRs with the ~ 1.4 $arcmin^2$ area outer shell of emission is less than 0.1%. Furthermore, the two components are very nearly centered at the same position (compare the cross and plus signs in Fig. 1). We are fairly confident that the two components are physically related. The interpretation of the age difference which we favor is that the Sedov solution is not applicable to the outer shell of emission. Recall that the Sedov solution assumes a homogeneous, isotropic medium for the expansion of the blast wave. Both the age and the energy estimates from the X-ray data would be decreased if the SN occurred within a preexisting low-density cavity in the ISM. In this case the initial expansion would be essentially free until the blast wave reached the wall of the cavity, at which point it would begin decelerating. The actual evolution depends on the interior density, the location of the inner edge of the cavity, the density of the cavity wall, and how the density varies through the jump at the cavity wall, and thus detailed numerical hydrodynamic simulations are necessary to determine energies and ages. However, from equation (2) we see that the ratio n/E_{51} should be less than 0.01 for the blast wave to propagate to $R \approx 12$ pc in less than 1000 yr. This then is a rough upper limit to the density of the cavity interior.

This scenario also resolves another apparent contradiction between the extremely large swept-up mass derived from the Sedov solution and the lack of complete thermalization of the ejecta (as evidenced by the existence of the oxygen filaments). Usually the reverse shock passes entirely through the ejecta after it has interacted with only 2–3 times its own mass. A low density within the cavity would be the alternative to requiring an extremely large ejected mass (~ 100 $M_\odot$) in the Sedov case. A cavity density as low as 0.01 cm^{-3}, though, would almost certainly require significant precursor mass loss at late stages of evolution in order to decelerate the ejecta and produce the observed X-ray and optical emission. The quasi-stationary knots seen in the optical near the center of the remnant are probably the relics of this mass-loss phase.

III. ANALYSIS OF THE HRI IMAGE

In § III*a* below, we examine the structure of the outer shell of emission, showing that it most likely arises from the interaction of the SN explosion with a cavity formed in the ISM by the pre–SN star. We also discuss (§ III*b*) the spatially resolved X-ray emission from the central region of N132D in light of the high-velocity oxygen-rich material observed at optical wavelengths and the O VIII Lyα X-ray line measured by the FPCS. Unfortunately, we are unable to pinpoint the spatial location of the O VIII Lyα emission region using the present data; the O VIII line may be coming predominantly from the central region, or it may be distributed uniformly throughout the whole remnant.

a) Outer Shell Emission

There are clear variations in surface brightness around the outer shell of the remnant. In the symmetric region the brightness at the shell varies from ~ 0.5 counts s^{-1} $arcmin^{-2}$ to greater than twice that. These differences can be accommodated for by density variations of $\sim 50\%$ or less in the emitting gas (see Table 1, col. [7]), variations which have little effect on the spherical shape of the remnant in this region. This can be seen by making recourse to the Sedov approximation and equation (2) in particular. Since $r \approx n^{-1/5}$, the radial dispersion due to density variations of 50% is $\Delta r/r \approx 7\%$. Thus for an assumed homogeneous ISM the symmetry of the southwestern region of the remnant (considering the range of brightness) is not remarkable. What is remarkable, however, is the region of the blowout toward the northeast, where the surface brightness is ~ 0.4 counts s^{-1} $arcmin^{-2}$ over almost a factor of 2 range in radii. This is shown in Figure 3, where we have plotted surface brightness (at the shell position) versus radial distance from the center of the symmetric region (assumed to be the location of

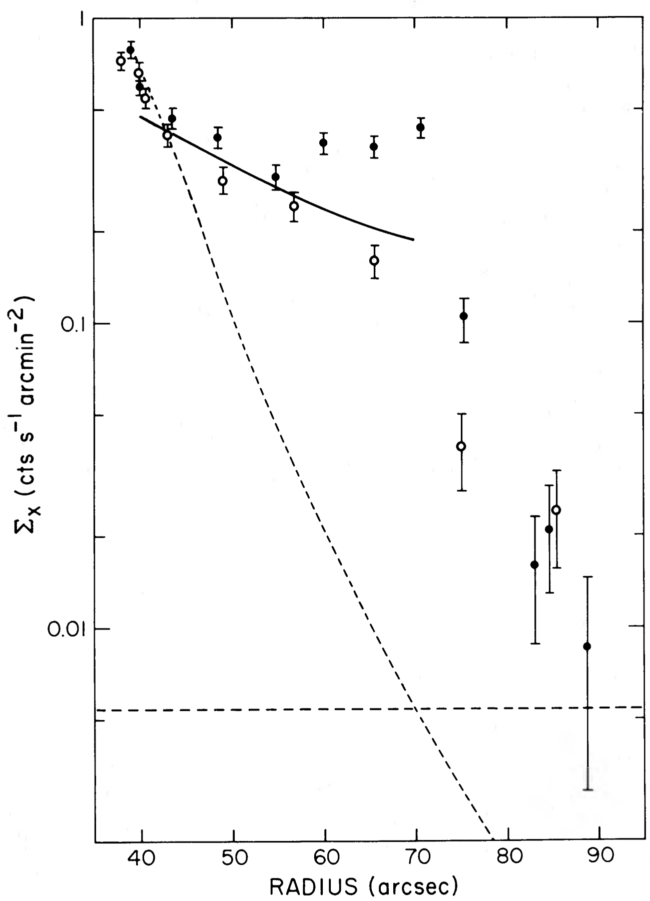

FIG. 3.—Plot of HRI surface brightness at the outer shell vs. distance from the center of the symmetric region for the eastern (*filled circles*) and northwestern regions (*open circles*) of N132D. The dashed line near the bottom is the average background level in the HRI field for this observation. The dashed curve represents the variation in Σ expected from either Sedov expansion in a homogeneous medium or expansion within the walls of a wind-blown cavity. The solid curve represents the variation in Σ expected from expansion within the walls of a photoionized cavity.

the explosion). The filled circles correspond to the eastern arm of the blowout (averages over the dotted boxes on the contour plot [Fig. 1]) and the open circles correspond to the northwestern arm (averages over the solid boxes in Fig. 1).

How could this observed structure have arisen? Perhaps the simplest possibility is that the ambient ISM density increases smoothly from the northeast to the southwest but is fairly homogeneous and uniform locally. In that case the blast wave would expand to greater size in the northeast than in the southwest as observed. Is this reasonable in detail though? The expansion in a region with large-scale inhomogeneities of this kind can be approximated by assuming Sedov expansion using different density values in different azimuthal sectors. The sound crossing time for this remnant, with $T \approx 10^7$ K and 10 pc, is $\sim$16,000 yr, so that the expansion toward either the NE or SW should be independent of the other. The Sedov relation between radius and density (eq. [2]) requires that if the expansion radius is a factor of 2 larger in one region from another, then the density must be less by a factor of $2^5 = 32$. The surface brightness (eq. [1]) varies as the square of the density, hence it must be a factor of $\sim 10^3$ less in the lower density (higher radius) region. This is shown graphically in Figure 3 where the dashed curve represents the variation in HRI surface brightness expected from the above scenario. It includes variations in the line of sight distance through the shell at different radii and assumes a constant shock temperature and hydrogen column density around the shell. In actuality the shock temperature should vary with radius as $T \approx r^2$ (compare eqs. [2] and [3]); this effect will decrease the expected emission in the HRI band for radii beyond 60″ from what we plot in Figure 3 (because of the nature of the HRI bandpass). However, this exercise is meant to be illustrative, not definitive; additional complications to the scenario arise from the three-dimensional nature of the hydrodynamic evolution of such a SNR, especially regarding the obliqueness of the shock front at the arms of the blowout. Our conclusion nevertheless is clear: there is too much X-ray brightness (by orders of magnitude) at radii of 70″–75″ than one would predict from this scenario.

Recently, two-dimensional hydrodynamic calculations of SNR evolution in the vicinity of a plasma density discontinuity have been carried out by various groups (Tenario-Tagle, Bodenheimer, and Yorke 1985; Falle and Garlick 1982). These calculations tend to support the above discussion in that large size differences around the remnant occur for large density differences. Our observations require fairly constant density differences for a large range of radii.

The major problem here is to decouple the density required for the dynamical evolution from the density derived from the observed surface brightness. One reasonable possibility is that there is a low-density medium filling a cavity within a higher density region. The low-density of the cavity interior allows the SN blast wave to expand rapidly to the walls where the transmitted shock produces the bulk of the X-ray emission and thereby decouples the dynamics from the observed brightness. On purely theoretical ground such cavities have been proposed, consistent with current ideas of stellar evolution and theories of the ISM (Shull *et al.* 1985; McKee, Van Buren, and Lazareff 1984; Weaver *et al.* 1977; Castor, McCray, and Weaver 1975).

In both scenarios considered below we assume as before that there was a preexisting smooth variation in the ambient ISM density, increasing from NE to SW. We then assume that the putative cavity was produced by either (1) the stellar wind of the precursor or (2) the H II region formed by its ultraviolet ionizing continuum radiation. The shape of the cavity, which directly determines the observed shape of the remnant, arises from the variations of expansion radius of the wind or H II region with varying density around the remnant. This is examined in detail below.

Castor, McCray, and Weaver (1975) have studied the interaction of a strong stellar wind with an homogenous ISM. They find a similarity solution for the radial evolution of the wind-blown shell, assuming no radiative losses, given by

$$R = 28\left(\frac{\dot{M}_6 V_{2000}^2}{n}\right)^{1/5} t_6^{3/5} \text{ pc} , \tag{4}$$

where $\dot{M}_6$ is the mass-loss rate in units of 10^{-6} $M_\odot$ yr^{-1}, V_{2000} is the wind speed in units of 2000 km s^{-1}, and t_6 is the period of stellar mass loss in units of 10^6 yr. In this scenario the wind sweeps up the ambient ISM into a thin dense shell with the interior of the shell filled by low-density ($n \approx 0.01$ cm^{-3}) gas. Equation (4) is quite similar in form to the radial expansion of a SNR in the Sedov solution (eq. [2]), and in fact the dependence of radius on density is the same ($r \approx n^{-1/5}$). The actual density at the cavity wall (which is now giving rise to the X-ray emission) depends principally on the thickness of the swept-up shell as well as possible effects of thermal conduction and radiation losses acting on the inside of the shell after the end of the mass-loss phase. However, as long as the relative shell thickness ($\Delta R/R$) does not depend strongly on the shell radius for azimuthal regions of different density, then the shell density is approximately proportional to the initial ambient density, viz., $n_f = (n_0/3)(R/\Delta R)$. Thus the variation in surface brightness with radius around the remnant is approximately the same as in the Sedov case above, which has already been shown to be unacceptable.

Next we consider the action of the stellar ionizing continuum on the surrounding ambient medium, assumed to increase from NE to SW as in the previous scenarios. In an homogeneous medium the Strömgren radius of the H II region formed about an early-type star of ionizing flux $10^{47}Q_{47}$ photon s^{-1} is given by

$$R = 14 n^{-2/3} Q_{47}^{1/3} \text{ pc} , \tag{5}$$

using $\alpha_B = 3 \times 10^{-13}$ cm^3 s^{-1} for the (optically thick, case B) hydrogen recombination rate (Osterbrock 1974). The mean density around the star is lowered because of the increased pressure of the H II region, which drives the surrounding matter into a thin dense shell at or near the radius given by equation (5). As in the stellar wind scenario, the shell structure, i.e., thickness and density, at the time of explosion will depend on physical processes acting on the shell during later phases of stellar evolution. Again we require that the relative shell thickness at different radii around the remnant be independent of density. If so, we obtain the solid line in Figure 3 for the surface brightness–radius variation.

This is a surpringly good qualitative fit to the data, particularly the NW arm of the blowout. The eastern arm is brighter than predicted over radii of 60″–70″ by factors of $\sim$2, which implies a local density enhancement of $\sim$50% or less. Indeed, a slightly higher density here is also supported by measurements of the obliqueness of the outer shell around the image. In each of the boxes in the contour plot of Figure 1, we define a local tangent to the shell (admittedly somewhat subjectively) using the local contours as guides. The obliqueness can then be measured as the angle between this normal and the radius vector to the box. In the NW the obliqueness increases smoothly from $\sim 90°$ (in the symmetric region) to $\sim 140°$ (at the outer edge of the arm). The situation is different in the east where the obliqueness increases from $\sim 90°$ (at the southernmost box) to a maximum of 140° but then decreases to $\sim 120°$ in the three boxes which correspond to the brighter region at radii of 60″–70″ in Figure 3. Even in the contour plot one can see how the eastern arm curves in slightly near its end, precisely the effect expected from a local density enhancement in this region.

As a consistency check we estimate the ionizing photon flux necessary to form a Strömgren sphere compatible with the observations. We can set limits on the original density surrounding the star, using the density values from Table 1 and limits on the shell thickness ΔR. Certainly the original density must be less than the present density of the shell divided by 4 (the strong shock compression factor), which is ~ 3 cm^{-3} or less. This is the limit of a thick shell. We have measured a lower limit to the shell thickness from Table 1, assuming that the shell must extend from R_i to R_o. This gives a lower limit to the ambient medium density of ~ 0.5 cm^{-3}. Using an approximate radius of 10 pc and the above densities gives a range for Q_{47} of $0.1 \leq Q_{47} \leq 3$, implying a progenitor no earlier than B0.

One further point regarding this hypothesis concerns the observation of an incomplete shell of low surface brightness optical emission at a radius of $\sim 2'$, seeming to cap the blowout region (Lasker 1978). This is at more than twice the radius of the outer shell in Figure 1. Lasker derives an emitting density from the Hα brightness of ~ 0.3 cm^{-3}. The 3 σ upper limit to the X-ray surface brightness in the same area is 0.003 counts s^{-1} arcmin^{-2}, which implies an upper limit of ~ 0.5 cm^{-3} to the density of any X-ray–emitting shell at a radius of 120″–150″. For a shock to propagate to this size, given the energy and age ranges from Figure 2, would require a density of at most 0.01–0.03 cm^{-3}. However, if the optical emission is arising from recombination in our proposed H II region then the flux of ionizing photons required (for $R = 32$ pc and $n = 0.3$ cm^{-3} in eq. [5]) is consistent with that derived above, $Q_{47} = 1.1$. In addition, this outermost shell may have been (re-)ionized by the UV blast of the SN; the ionization energies are consistent with that expected from type II SNs (Lasker 1978). Furthermore, this outer shell appears to be similar to the high-excitation photoionized halo around SNR 0102−72.3, an oxygen-rich SNR in the Small Magellanic Cloud (Dopita, Tuohy, and Mathewson 1981; Tuohy and Dopita 1983).

We close this section with a discussion of the possible modifications to the above results with the inclusion of current theories concerning the inhomogeneous nature of the ISM. First we note that the large limb-brightening of the outer shell (as much as 4:1) argues against the evolution of the remnant into an uniformly inhomogeneous region as examined in Cowie, McKee, and Ostriker (1981). The dramatic lack of spherical symmetry is also problematic since the dynamical evolution in a cloudy medium is regulated by the highest filling factor component, which is the (supposed constant) hot intercloud gas of density 1.6×10^{-3} cm^{-3} (McKee and Ostriker 1977). However, a cavity, as proposed above, from which clouds had been evacuated would be quite consistent with the observations, while the coincidence of X-ray and optical emission in the outer shell almost certainly requires the presence of clouds there. Approximate pressure equilibrium exists between the X-ray shell [$p/k \approx (2\text{–}14) \times 10^7$ K cm^{-3}] and the optical knots at the shell (e.g., $p/k \approx 2 \times 10^7$ K cm^{-3} for Lasker's knot No. 13).

How does an inhomogeneous medium affect our conclusions concerning progenitor type? It strengthens our requirement of a progenitor star later than B0. McKee, Van Buren, and Lazareff (1984) find that early-type stars form cavities in the ISM of radii $56 n_m^{-0.3}$ pc, where n_m is the mean initial circumstellar density. For the (shell) density values from our HRI observations, the calculated radius is several factors of 2 larger than observed, implying that the progenitor could not have been earlier than B0. This is now the third SNR for which a B0-type progenitor has been proposed, the others being N49 in the LMC (Shull *et al.* 1985) and the Cygnus Loop (Charles, Kahn, and McKee 1985). However, we feel that the evidence presented here for N132D makes perhaps the best case for the scenario of an explosion within a cavity. Below, we turn our attention to the central regions of the remnant which contain the high-velocity oxygen-rich material.

b) *Central Emission*

In several respects the central part of this remnant is the most interesting. This is where the optical observations reveal a high velocity ring of oxygen-rich plasma, some of which corresponds to regions of bright X-rays. We explore the possibility that much of the central X-ray emission is coming from oxygen-rich plasma, although we are unable to determine this definitively at the present time.

As mentioned earlier, the central X-ray emission appears to be concentrated toward the north and west (see Fig. 1). The eastern region is remarkably less luminous in X-rays and in fact contributes only $\sim 2\%$ to the total central emission (see below). In this area the optical knots appear to be moving at speeds of 1700–3400 km s^{-1} (Danziger and Dennefeld 1976), which are some 2–3 times larger than the recession velocities measured in the western region, and which may imply an inclined ring geometry (Lasker 1980). However, we note that this is also consistent with the apparent lack of significant amounts of slow-moving gas toward the east (compared to the bright optical knots in the west and particularly the north) and may be indicating less efficient deceleration of the stellar ejecta in this direction.

We now turn to a discussion of the central X-ray emission itself. Estimating the luminosity from this region is complicated by the fact that we observed it through the outer shell of emission. Our approach was to subtract off the expected central emission from the appropriate outer spherical shell (using the best-fit values in Table 1) for each azimuthal sector. This is reasonable for the spherical region, but it overestimates the central emission in the region of the blowout. Here we are seeing through increasingly more outer emission as we progress from the blowout in toward the center. In this region we assumed a monotonic linear decrease in (outer shell) surface brightness from the center (fixed at the central surface brightness of the spherical region ~ 0.3 counts s^{-1} arcmin^{-2}) to beyond where the central emission ends at $\sim 40''$. Note that this linear extrapolation fits the observed brightness profile from 40″–70″.

The count rate so derived for the whole central region is 0.13

HRI counts s^{-1} with an estimated error of $\sim 20\%$ or less, arising from our procedure for subtracting emission from the outer shell. This is 10% of the total HRI emission from N132D, and aside from itself, only eight of the 30 or so other remnants in the LMC are brighter than this. About 70% of the emission comes from the northern filament and the remainder from the western one. The peak brightness of the northern filament is ~ 0.5 counts s^{-1} arcmin^{-2} after subtracting the outer shell contribution. It has a thickness in the plane of the sky of $\sim 10''$ and a length of $\sim 30''$, which implies a volume of 1.3×10^{57} cm^3 for an assumed cylindrical geometry. We can estimate the emitting density from the HRI profile as above and we find $n \approx 4$–5 cm^{-3} for a solar abundance plasma at temperatures $10^{6.8}$–$10^{7.1}$ K; this yields a mass of 6–8 $M_\odot$ for the filament (however, see caveats below).

However, two clues lead us to consider possible overabundance of oxygen in the central region: (1) the high-velocity oxygen-rich ring observed in the optical and (2) the bright O VIII Lyα line observed in the global X-ray spectrum. For a cosmic abundance plasma of temperatures $10^{6.8}$–$10^{7.2}$ the fraction of emission in the HRI bandpass from this oxygen line is only 2%–4% (for a column density of $\sim 2 \times 10^{21}$ cm^{-2}), more than a factor of 2 less than observed by the FPCS. Oxygen must be overabundant in the remnant; but whether the oxygen is distributed uniformly through the remnant or concentrated in the central regions cannot be determined by the present X-ray data.

However, let us explore the consequences of assuming that the oxygen abundance in the outer shell is at its cosmic value. In that case the central regions must be overabundant in oxygen, in such a way that they supply $\sim 7\%$ of the total X-ray luminosity of the remnant in the single O VIII Lyα line. Since the central regions contribute only 10% of the total luminosity anyway, this means that 70% of the emission from the center must be in the O VIII Lyα line. This requirement is difficult to satisfy even with a pure oxygen plasma (assuming equilibrium ionization), where the fractional contribution of the O VIII Lyα line is 0.59–0.69 in the HRI bandpass for temperatures from $10^{6.6}$–$10^{7.0}$ and $N_H = 2 \times 10^{21}$ atoms cm^{-2}. Effects of nonequilibrium ionization, as well as any underabundance of iron in the outer shell of the SNR, may mitigate this requirement. In a later paper we will examine these possibilities in light of the spectral observations; i.e., the FPCS and SSS data and a nonequilibrium ionization model (Hughes and Helfand 1985). As an approximate lower limit to the mass in this filament we assume that it consists of pure oxygen. This implies a density of oxygen atoms of 0.05–0.1 cm^{-3} and a corresponding mass range of 1–2 $M_\odot$ (of oxygen) for the same cylindrical geometry used above. As a caveat we must stress that these mass values (and the ones for a solar abundance plasma) are quite uncertain for various reasons. They are derived assuming a uniform density; any clumpiness will lower the derived masses by a factor $f^{1/2}$, where f is the volume filling factor occupied by the X-ray–emitting plasma. The elemental abundances and ionization states are unknown. Finally, unheated ejecta surely must be present interior to the position of the reverse shock.

IV. CONCLUSIONS

We have examined the X-ray morphology of the LMC SNR N132D and have determined that it most probably arises from the interaction of the SN blast wave with a cavity in the ISM. The structure of the cavity is consistent with having been formed by the H II region of the SN precursor star, whose type we estimate to be later than B0. This scenario reduces the explosion energy $[2.3 \leq E(10^{51}\ \text{ergs}) \leq 11.4]$ and age $[4300 \leq t(\text{yr}) \leq 7200]$ derived from the Sedov similarity solution and allows for consistency with the expansion age of the oxygen-rich optical filaments (~ 1300 yr). In future work we will consider the evolution of SNRs in such a cavity, exploring the effects of varying the interior density, cavity radius, and structure of the inner edge of the cavity.

We have also briefly discussed the emission from the central region of the remnant, which contributes $\sim 10\%$ to the total X-ray emission from the remnant (in the HRI bandpass). Since this position in the SNR corresponds to locations of bright oxygen-rich optical knots we have considered the possibility that the X-rays are coming from oxygen enriched plasma as well. However, assuming normal cosmic abundances in the outer shell almost surely requires a pure oxygen plasma for the central regions to account for the O VIII Lyα line observed by the FPCS. On the other hand, this conclusion depends sensitively on the assumed abundance of iron throughout the remnant; future work with the FPCS and SSS spectral observations may help determine this. Our very rough mass estimates (certainly upper limits) for the material in the center ($\lesssim 10$ $M_\odot$) are consistent with the total mass of a B0 or slightly later type star, at least implying consistency with our earlier results on the outer shell emission.

We note that the presence of high-velocity oxygen-rich optical filaments as well as X-ray emission in the central regions of the remnant suggest that the ejecta have not yet interacted with a significant amount of circumstellar matter. Using the standard Sedov picture for SNR evolution in a uniform medium, we have shown that the ejecta would have interacted with several hundred solar masses of swept-up material. In this case, unless the ejected mass were on the order of 100 $M_\odot$ or so, we would expect it to be fully thermalized. However, in the low-density cavity scenario, the residual mass in the cavity would probably be too low to drive a reverse shock into the ejecta of sufficient strength to produce the observed central emission. At a density of 0.01 cm^{-3}, there is less than 0.03 $M_\odot$ within the 3 pc radius central ring. But stars of 1 $M_\odot$ or greater during their post–main-sequence evolution can lose significant amounts of mass in a low-velocity stellar wind (Knapp *et al.* 1982). It is not unreasonable, for a B0 progenitor, to expect several solar masses of wind material within the 3 pc central region. Once the SN occurred, this material would decelerate a comparable mass of ejecta. The best evidence for this is the presence of slow moving optical knots with enhanced abundances of oxygen and sulfur observed near the center of the remnant (Lasker 1978; Danziger and Leibowitz 1985).

This remnant has consistently stood out in previous X-ray studies as being much brighter for its size than the rest of the LMC sample of SNRs (see Hughes 1984). In this paper we present evidence that this object is unique from most other remnants in at least two ways: (1) in having X-ray emission from central material, presumably to be identified with stellar ejecta and (2) in having exploded within a cavity in the ISM. Both of these effects tend to increase the remnant's brightness for its size in comparison to other SNRs. Continued detailed work on the X-ray morphology of the LMC SNRs will certainly lead to more interesting results and allow a better understanding of the various ways that SNRs interact with their environment.

We thank Claude Canizares and his colleagues at the Center for Space Research for supplying us with the results of the FPCS observations. We also acknowledge the hospitality of the Aspen Center for Physics and the Institute of Space and Astronautical Science, Tokyo, Japan, where the writing of this paper was begun and finished, respectively. Thanks are also extended to Karen Modestino for her care with this manuscript. We appreciate the useful suggestions of the referee, Michael Dopita.

REFERENCES

Canizares, C. R. 1985, private communication.
Castor, J., McCray, R., and Weaver, R. 1975, *Ap. J. (Letters)*, **218**, 377.
Charles, P. A., Kahn, S. M., and McKee, C. F. 1985, *Ap. J.*, **295**, 456.
Clark, D. H., Tuohy, I. R., Long, K. S., Szymkowiak, A. E., Dopita, M. A., Mathewson, D. S., and Culhane, J. L. 1982, *Ap. J.*, **255**, 440.
Cowie, L. L., McKee, C. F., and Ostriker, J. P. 1981, *Ap. J.*, **247**, 908.
Cox, D. P., and Franco, J. 1981, *Ap. J.*, **251**, 687.
Danziger, I. J., and Dennefeld, M. 1976, *Ap. J.*, **207**, 394.
Danziger, I. J., and Leibowitz, E. M. 1985, *M.N.R.A.S.*, **216**, 365.
Dopita, M. A., Tuohy, I. R., and Mathewson, D. S. 1981, *Ap. J. (Letters)*, **248**, L105.
Falle, S. A. E. G., and Garlick, A. R. 1982, *M.N.R.A.S.*, **201**, 635.
Hughes, J. P. 1984, Ph.D. thesis, Columbia University.
Hughes, J. P., and Helfand, D. J. 1985, *Ap. J.*, **291**, 544.
Knapp, G. R., Phillips, T. G., Leighton, R. B., Lo, K. Y., Wannier, P. G., Wootten, H. A., and Huggins, P. J. 1982, *Ap. J.*, **252**, 616.
Lasker, B. M. 1978, *Ap. J.*, **223**, 109.
———. 1980, *Ap. J.*, **237**, 765.
Markert, T. H., Canizares, C. R., Pfafman, T., Vedder, P., Winkler, P. F., and Pradhan, A. 1984, in *IAU Colloquium 86, Ultraviolet and X-Ray Spectroscopy of Astrophysical and Laboratory Plasmas*; chairperson, G. A. Doschek (Washington, DC: Naval Research Laboratory), p. 76.
Mathewson, D. S., Ford, V. L., Dopita, M. A., Tuohy, I. R., Long, K. S., and Helfand, D. J. 1983, *Ap. J. Suppl.*, **51**, 345.
McKee, C. F., and Ostriker, J. P. 1977, *Ap. J.*, **218**, 148.
McKee, C. F., Van Buren, D., and Lazareff, B. 1984, *Ap. J. (Letters)*, **278**, L115.
Osterbrock, D. E. 1974, *Astrophysics of Gaseous Nebulae* (San Francisco: Freeman).
Raymond, J. C., and Smith, B. W. 1977, *Ap. J. Suppl.*, **35**, 419.
Sedov, L. I. 1959, *Similarity and Dimensional Methods in Mechanics* (New York: Academic Press).
Shull, P. Jr., Dyson, J. E., Kahn, F. D., and West, K. A. 1985, *M.N.R.A.S.*, **212**, 799.
Tenorio-Tagle, G., Bodenheimer, P., and Yorke, H. W. 1985, *Astr. Ap.*, **145**, 70.
Tuohy, I. R., and Dopita, M. A. 1983, *Ap. J. (Letters)*, **268**, L11.
Weaver, R., McCray, R., Castor, J., Shapiro, P., and Moore, R. 1977, *Ap. J.*, **218**, 377.

JOHN P. HUGHES: Harvard-Smithsonian Center for Astrophysics, 60 Garden Street, Cambridge, MA 02138